From atomic semimetal to topological nontrivial insulator

Xiao-Ping Li,[1,2] Da-Shuai Ma,[3,1,2,*] Cheng-Cheng Liu,[1,2] Zhi-Ming Yu,[1,2] and Yugui Yao[1,2,†]

[1]*Centre for Quantum Physics, Key Laboratory of Advanced Optoelectronic Quantum Architecture and Measurement (MOE), School of Physics, Beijing Institute of Technology, Beijing 100081, China*

[2]*Beijing Key Laboratory of Nanophotonics and Ultrafine Optoelectronic Systems, School of Physics, Beijing Institute of Technology, Beijing 100081, China*

[3]*Chongqing Key Laboratory for Strongly Coupled Physics and Institute for Structure and Function, Department of Physics, Chongqing University, Chongqing 401331, China*

(Received 21 September 2021; accepted 7 April 2022; published 19 April 2022)

Topological band insulators and (semi-)metals can arise out of atomic insulators when the hopping strength between electrons increases. Such topological phases are separated from the atomic insulator by a bulk gap closing. In this paper, we show that in many (magnetic) space groups, the crystals with certain Wyckoff positions and atomic orbitals being occupied must be semimetals in the atomic limit, e.g., the hopping strength between electrons is infinitesimal but not vanishing, which then are termed atomic semimetals (ASMs). We derive a sufficient condition for realizing ASMs in both spinless and spinful systems. Remarkably, with both symmetries and electron fillings of system preserved, increasing the hopping strength between electrons may transform an ASM into an insulator, and the induced insulators inevitably are topologically nontrivial. Particularly, using silicon as an example, we show the ASM criterion can discover the obstructed atomic insulators (OAIs) that are marked as trivial insulators on the topological quantum chemistry website. Our paper not only establishes an efficient way to identify and design topologically nontrivial insulators, but also predicts that the group-IV elemental semiconductors are ideal candidate materials for OAI.

DOI: 10.1103/PhysRevB.105.165135

I. INTRODUCTION

The past decade has witnessed the prosperity and development of the band topology in condensed-matter physics [1–4]. The topology in electronic bands has been recognized for a long time, such as the quantum Hall effect and the quantum anomalous Hall effect [5,6]. However, in the early stage the topological phases in crystals were considered very rare and required strict external conditions [7]. The discovery of the topological insulator and the topological Weyl semimetal open up a new direction for realizing topological phases in noninteracting systems by exploring spin-orbit coupling (SOC) effect [8–10]. Many materials constructed by heavy atoms are predicted as topological materials with nontrivial boundary states [11–25]. However, compared with the realistic materials in the database, the number of the topological materials is still very small.

The breakthrough comes from the establishment of several equivalent theories: topological quantum chemistry (TQC) [26,27], symmetry indicator theory [28–30], and related theories [31–33], all of which present a quantitative description of the atomic insulators, respectively, based on the elementary band representations (EBRs) and the symmetry eigenvalues of the bands at high-symmetry points. The application of these two theories to the material database predicted that thousands of realistic materials are topologically nontrivial [34–37]. However, there is a caveat for the classification due to the definition of the topologically trivial insulator. In the definition, the topologically trivial insulator is the material that its band representation (BR) of valence bands can be represented by a sum of EBRs [26], which means the trivial state can be described by a set of exponentially localized Wannier functions [38]. Furthermore, based on the Wyckoff positions where the orbitals that induce the BRs are locating at, the trivial insulator can be divided into two classes, i.e., obstructed atomic insulators (OAIs) and atomic insulators. For atomic insulators, the BRs are induced from the orbitals locating at occupied Wyckoff positions. However, for OAIs, the BRs cannot be induced only from the orbitals centered at the occupied Wyckoff positions, but also need orbitals locating at empty sites [26,38–41]. Phases that are inequivalent to atomic insulator including stable topological insulator, fragile topological insulator (FTI), and OAI are *topologically nontrivial*. Remarkably, one can find out the surface states of OAIs in certain surface where the Wannier centers can be cut as terminal [42–45].

Meanwhile, the group-IV elemental semiconductors, such as silicon (Si), diamond, and germanium, play a central role in the modern microelectronics industry. These elementary materials are widely studied and were considered as topologically trivial semiconductors with an indirect band gap due to negligible SOC and a sizable band gap. According to both the database [44] and filling-enforced OAI [45], the group-IV elemental semiconductors indeed are classified into topologically trivial insulators. However, a recent study shows the silicon has a surface state [46–48], similar to the OAI.

*madason.xin@gmail.com
†ygyao@bit.edu.cn

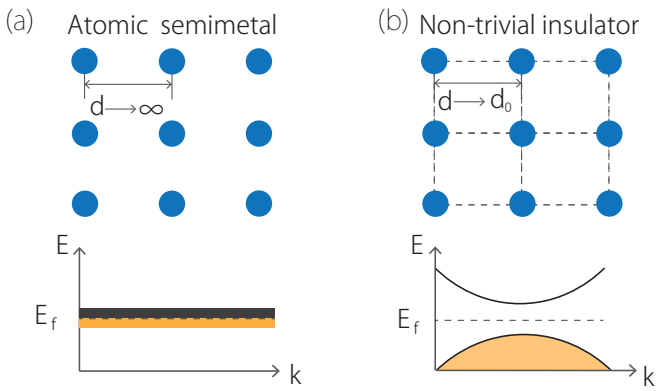

FIG. 1. (a) and (b) Schematic of the crystal structure in the atomic limit and crystal phase. The occupied bands are highlighted in yellow. See Fig. 3 for silicon as a specific example.

Thus, several natural questions arise: Does the silicon and the other group-IV elemental semiconductors be OAI? If they are, then does there exist an efficient method to identify OAIs? And even more, is there a sample approach to identify all of the topologically nontrivial phases without the time-consuming density functional theory (DFT) calculations?

In this paper, we address these questions in the affirmative. We point out that, for many crystals with certain Wyckoff positions and orbitals being occupied, they must be (semi-)metal, i.e., atomic semimetal (ASM) when the hopping strength between electrons is infinitely weak but not vanishing due to the presence of partially filled EBRs [see Fig. 1(a)]. By increasing the hopping strength, the systems can be transformed into insulators due to band inversion when both symmetries and electron fillings of the crystal are preserved as illustrated in Fig. 1(b). The insulators transformed from atomic semimetal must be topologically nontrivial due to inequivalence between such an insulator phase and the atomic limit semimetal phase. For example, the topological crystalline insulator (TCI) SnTe can be emerged from ASM. Since the stable and fragile topological insulators have been presented on the TQC website, here, we focus on the emerging of OAIs from ASMs. In other words, materials classified as trivial insulator should be OAIs if they are ASMs. We also present a sufficient condition for the ASMs in spinless and spinful systems, which only depend on the crystal structure and the orbitals of the atoms. Thus, using the condition of ASM to diagnose OAI will be very efficient as it is independent of the DFT calculations. By applying the criterion to the group-IV elemental semiconductors, we find they fall into the condition of ASM, indicating that they would be OAI rather than a trivial semiconductor. This result is further confirmed by DFT calculations. Particularly, the condition of ASM also offers useful guidance for designing topological states with light atoms as in such a case no matter whether the system is a semimetal or an insulator, it must be topologically nontrivial.

II. CONDITION OF ATOMIC SEMIMETAL

We consider a three-dimensional material system belonging to (magnetic) space-group $\boldsymbol{G}$. The atoms in this system can be divided into N nonequivalent sets, and the ith

TABLE I. The atomic orbitals and IRRs of the T_d point group. The third column are the BRs induced by the corresponding atomic orbitals in 8a Wyckoff position of the 227 space group.

Orbital	IRRs	BRs
s ($l=0$)	A_1	$A_1 \uparrow \boldsymbol{G}(2)$
p ($l=1$)	T_2	$T_2 \uparrow \boldsymbol{G}(6)$
d ($l=2$)	$E \oplus T_2$	$E \uparrow \boldsymbol{G}(4) \oplus T_2 \uparrow \boldsymbol{G}(6)$
f ($l=3$)	$A_1 \oplus T_1 \oplus T_2$	$A_1 \uparrow \boldsymbol{G}(2) \oplus T_1 \uparrow \boldsymbol{G}(6) \oplus T_2 \uparrow \boldsymbol{G}(6)$

($i = 1,2,...,N$) set of atoms can be labeled as $\{i; w_i, \sum_l O_l^{n_l}\}$ where w_i denotes the occupied Wyckoff position. (Here we assume that if the coordinates of Wyckoff position depend on the parameters, the value of i is different for changing the parameters), O_l is the atomic orbital of the atom with (total) angular momentum l, and n_l is the number of electrons residing at the corresponding orbital. For spinless systems, $l = 0, 1, 2\cdots$ is an integer, and for spinful systems, $l = \frac{1}{2}, \frac{3}{2}\cdots$ is a half odd integer. Assuming the site symmetry of the w_i Wyckoff position is $\boldsymbol{g}_{w_i}$, and the mth irreducible representations (IRRs) of $\boldsymbol{g}_{w_i}$ are $\rho_{w_i}^{m=1,2\cdots}$. The atomic orbital O_l of the atom at w_i generally would be splitted into different IRRs ($\rho_{w_i,l}^m$) of $\boldsymbol{g}_{w_i}$ by the crystalline field with symmetry of $\boldsymbol{g}_{w_i}$. For example, in spinless systems the five $l = 2$ (d) orbitals would be two levels, represented two IRRs E and T_2 by the crystalline field with symmetry of the T_d point group as listed in Table I. According to TQC, the IRRs $\rho_{w_i,l}^m$ in space-group $\boldsymbol{G}$ can be expressed as $\rho_{w_i,l}^m \uparrow \boldsymbol{G}$, for which the dimension is denoted as $d(\rho_{w_i,l}^m \uparrow \boldsymbol{G})$. Then a sufficient condition for a system to be an atomic semimetal phase is equivalent to there does not exist a solution for the following equation:

$$N_{\text{occ}} = \chi \sum_{i,l,m} c_{i,l,m} d\left(\rho_{w_i,l}^m \uparrow \boldsymbol{G}\right), \qquad c_{i,l,m} \in \{0, 1\}, \quad (1)$$

where N_{occ} is the total number of the electrons of the material and $\chi = 2$ for spinless systems and $\chi = 1$ for spinful systems. Note that the summation in Eq. (1) is constrained in the occupied Wyckoff position and the occupied atomic orbitals. Besides, whereas the ASM also is filling enforced, it cannot be fully captured by the theory proposed by Watanabe *et al.* [49] as the ASM predicted here can be transformed into a gapped state with maintaining the electron fillings as shown in the following discussion of silicon. Particularly, the criterion of the vASM is quite different from that of the filling enforced OAI where the occupied Wyckoff positions always have higher multiplicity than that of a *necessary* empty Wyckoff position. Thus, applying the criterion of ASM that was built upon the theory of EBRs to the trivial insulators in TQC database can discover the OAIs that cannot be diagnosed by the criterion of the filling enforced OAI. The proposal of ASM is fundamentally interesting in that it shows the hopping strength of electrons can transform semimetal phase into topologically nontrivial insulator phase. This also indicates that all the material systems fall into the ASM criterion would be topologically nontrivial as they inevitably cannot be adiabatically transformed into atomic insulator without a gap closing or opening.

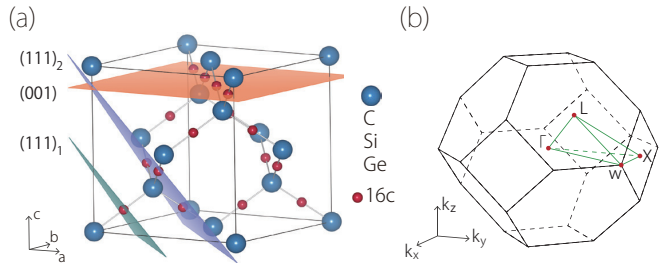

FIG. 2. (a) Crystal structure of group-IV elemental semiconductor materials. The Wannier charge centers are denoted by small red balls located at Wyckoff position 16*c*. The three kinds of surface termination, e.g., $(111)_1$, (001), and $(111)_2$ are highlighted in green, blue, and orange, respectively. (b) Bulk Brillouin zone (BZ) of group-IV elemental semiconductor materials.

III. SILICON AND ASM-INSULATOR TRANSITION

We take Si as an example to check the ASM criterion and study the hopping strength-driven ASM-insulator transition. Since the SOC effect of Si is negligible, the bulk silicon can be considered as a spinless system. Moreover, the bulk silicon is well known to have a tetrahedral crystal structure with space-group $Fd3m$ (No. 227) as shown in Fig. 2(a). Each unit cell of elemental Si contains eight Si atoms with perfect tetrahedral $sp3$ bonding residing at the Wyckoff position 8*a*, and there are two Si atoms in each primitive unit cell. Thus, the multiplicity of Wyckoff position 8*a* whose site symmetry group is T_d, and the point group is 2 for the primitive unit cell. The arrangement of electrons of the Si atom in the outer shell is $3s^2 3p^2$, indicating the total number of electrons in a primitive unit cell of silicon is 8. According to the crystalline-field splitting, the IRRs from the *s* and *p* orbitals at 8*a* are A_1 and T_2 (e.g., $\rho^1_{8a,l=0} = A_1 \uparrow \boldsymbol{G}$ and $\rho^5_{8a,l=1} = T_2 \uparrow \boldsymbol{G}$), respectively. From Ref. [50], one knows the dimension of the two IRRs induced from A_1 and T_2 orbitals are $d(A_1 \uparrow \boldsymbol{G}) = 2$ and $d(T_2 \uparrow \boldsymbol{G}) = 6$. According to Eq. (1), we immediately have

$$\nexists c_{i,l,m} \in \{0, 1\}, \quad \text{such that } 8 = 2(2c_{1,0,1} + 6c_{1,1,2}), \quad (2)$$

showing that in the atoms limit the silicon must be a semimetal as illustrated in Figs. 3(a) and 3(c).

However, as we know the pristine silicon is a semiconductor [see the band structure of silicon in Fig. 3(d)], and then there would exist a strain-driven ASM-insulator transition in silicon. To directly demonstrate it, we calculate the electronic properties of silicon under different tensile stresses. The results and the obtained phase diagram are shown in Fig. 3(e). Without stress, the silicon is calculated as a semiconductor as it should be. By applying stress, the band gap at the Γ point will decrease and finally closes under ∼11% tensile stress. The band inversion occurring at Γ leads to a semimetal state for the silicon. Keep increasing tensile, there does not exist another phase transition, namely, the silicon under the atomic limit is a semimetal state, consistent with the above analysis. Moreover, by calculating the BRs of the silicon under 40% stress, we find that the BR of the lower eight bands (four valence bands and four conduction bands) indeed are induced by the *s* and *p* orbitals at the 8*a* position, and a clear diagram of band inversion is shown in Figs. 3(a) and 3(b).

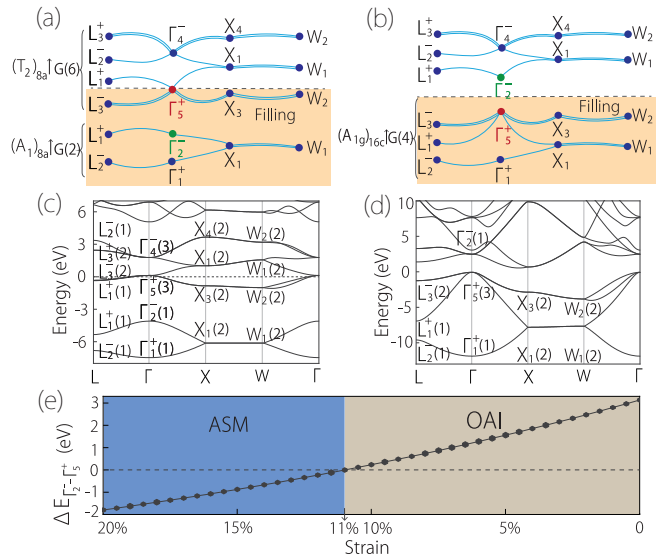

FIG. 3. (a) Schematic of the EBRs $(A_1)_{8a} \uparrow G(2)$ and $(T_2)_{8a} \uparrow G(6)$ induced from *s* and *p* orbitals at Wyckoff position 8*a* with eight electrons (four bands are occupied in the spinless case). (b) Schematic of the EBRs that undergo a band inversion between $\Gamma_2^-(1)$ and $\Gamma_5^+(3)$. (c) The band structure of silicon under 40% tensile stress. (d) The band structure of silicon with the fully optimized lattice constant. The BRs of bands at the high-symmetry points are also given. The superscript ± denotes the parity. (e) The phase diagram and band gap between $\Gamma_2^-(1)$ and $\Gamma_5^+(3)$ as a function of the lattice constant.

IV. OAI AND FLOATING SURFACE STATES

Since the semiconductor state of silicon is transformed from ASM, pristine silicon would be topologically nontrivial. According to the database of TQC and Ref. [45], silicon does not have stable and fragile topologies. Thus, one can expect that the silicon would be an OAI. To confirm it, we calculate the BRs of the valence bands of pristine silicon [see Fig. 3(d) and details in the Appendices] and find the BRs are solely induced by the A_{1g} orbital in the D_{3d} point group at Wyckoff position 16*c* of space-group $Fd3m$, which is an unoccupied position in silicon. In Fig. 2(a), we also marked the 16*c* Wyckoff position with red and small balls. In other words, there is obstructed Wannier charge centers locating at the Wyckoff position 16*c*. Hence, the result directly demonstrates that silicon is an OAI.

We then study the surface state of silicon. Distinguished from the Chern insulator and topological insulator where the surface states always cross the bulk gap regardless of the boundaries, the surface states of OAI are floating bands appearing in the bulk gap and only occur on the boundaries that cut through the unoccupied Wyckoff position where the Wannier charge centers is locating at. This means that whereas the surface state of OAI is not as robust as that in the Chern insulator and topological insulator, which indicates that the floating surface state in OAI can be tunable under suitable perturbations. Interestingly, when we chose the three crystal planes labeled as $(111)_1$, (001), and $(111)_2$ planes in Fig. 2(a) as cleavage terminations, there would exist three completely different surface states on the corresponding boundaries.

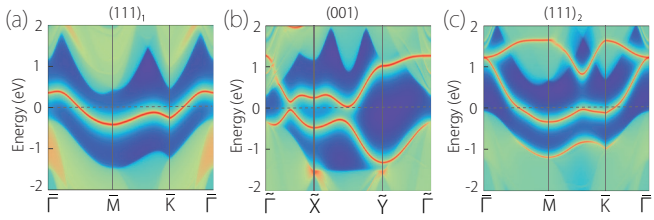

FIG. 4. (a)–(c) Surface spectra on $(111)_1$, (001), and $(111)_2$ surfaces. The surface Brillouin zone and paths of surface bands are provided in the Appendices.

The calculated surface states of silicon for the three boundaries are plotted in Figs. 4(a)–4(c). One finds that $(111)_1$, (001), and $(111)_2$ boundaries exhibit one–three floating surface bands, respectively. This is because the three boundaries cut one–three obstructed Wannier charge centers [see Fig. 2(a)].

Since the mismatch between the obstructed Wannier charge centers and the atom's position can lead to a bulk electric polarization, the floating surface states can also be understood in terms of the Zak phase along a straight line normal to the boundary. The expression of Zak phase generally can be expressed as [51]

$$\mathcal{Z}(\boldsymbol{k}_\parallel) = -i \sum_n \int_0^{2\pi} \left\langle u_{n\boldsymbol{k}} \left| \frac{\partial}{\partial k_\perp} \right| u_{n\boldsymbol{k}} \right\rangle dk_\perp, \tag{3}$$

where the summation is performed on the occupied bands, $\boldsymbol{k}_\parallel$ ($\boldsymbol{k}_\perp$) denotes the momentum parallel (normal) to the boundary, and $|u_{n\boldsymbol{k}}\rangle$ is the lattice periodic part of the Bloch wave function. For the Zak phases $\mathcal{Z}(\boldsymbol{k}_\parallel)$ of a straight line normal to $(111)_1$ and $(111)_2$ boundaries, it is calculated as π for any $\boldsymbol{k}_\parallel$, showing the nontrivial properties of silicon. However, the Zak phase $\mathcal{Z}(\boldsymbol{k}_\parallel)$ of a straight line normal to the (001) boundary is calculated as 0 for any $\boldsymbol{k}_\parallel$. The inconsistency between the trivial Zak phase and the two floating surface bands on the (001) boundary is due to the fact the Zak phase is a $\mathbb{Z}_2$ topological quantum number and cannot capture the topological nature of systems with even floating surface bands. Therefore, for the prediction of the floating surface bands of OAIs, the obstructed Wannier charge centers calculated by TQC are more advantageous and can provide more accurate information.

V. DISCUSSION AND CONCLUSION

The group-IV elemental materials, such as diamond, silicon, germanium, and tin, have the same crystal structure and similar arrangement of electrons in the outer shell, e.g., ns^2np^2 with $n = 2$–5 for C, Si, Ge, and Sn atoms, respectively. Hence, all the group-IV elemental materials satisfy the criterion of ASM and are topologically nontrivial, except that group-IV elemental semiconductors, e.g., diamond, silicon, and germanium are OAI, whereas Sn naturally is in the ASM phase.

It should be noted that Eq. (1) is a sufficient but not a necessary condition for the ASM. To obtain a sufficient and necessary condition for ASM, one should have the information of the energy level of all the induced BRs, which cannot be inferred from the crystalline structure and the atomic orbitals. One possible way to find out all the topological materials satisfying the ASM criterion is to calculate the band structure of each realistic material in the database under sufficiently large tensile stress and check whether it is gapless or not. Besides, since there does not exist a sufficient and necessary condition for diagnosing all the possible topological materials, comparing the BRs induced by the valence band of each realistic material with a sufficiently large tensile stress and the BRs of the corresponding material without stress may be a possible effective method to address this task.

To summarize we propose the concept of the ASM and establish a sufficient condition for ASM. We find s group-IV elemental semiconductor: silicon satisfies the ASM criterion and then would be topologically nontrivial. Further calculations show silicon is an OAI. Based on the location of obstructed Wannier charge centers, we also discuss the floating surface states for three different boundaries of silicon, which presents a quantitative and physical description of the surface states of silicon. Due to mature theology, silicon would be the most ideal material for studying much more novel phenomena associated with OAI. Moreover, the criterion of ASM is a very powerful tool that cannot only identify topological nontrivial phases, but also be used to design topological materials by placing specific atoms at Wyckoff positions in a given space group.

ACKNOWLEDGMENTS

This work was supported by the National Key R&D Program of China (Grant No. 2020YFA0308800), the NSF of China (Grants No. 11734003, No. 12061131002, No. 12004035, No. 11922401, and No. 11774028) and the Strategic Priority Research Program of the Chinese Academy of Sciences (Grant No. XDB30000000).

APPENDIX A: METHODS

The first-principles calculations are performed based on the DFT using the Vienna *ab initio* simulation package [52,53]. The exchange-correlation potential is taken within the generalized gradient approximation of Perdew-Burke-Ernzerhof type [54] and the projector augmented-wave pseudopotential [55] in the main text. The cutoff energy is set as 500 eV, and Γ-centered k mesh with size $16 \times 16 \times 16$ are used for the primitive cell. The energy and force convergence criteria are set to be 10^{-7} eV and 10^{-3} eV/Å, respectively. The surface states are calculated by constructing the maximally localized Wannier functions [56] via the WANNIERTOOLS package [57] based on the iterative Green's function method. In this Appendix, the more sophisticated Heyd-Scuseria-Ernzerhof hybrid functional method (HSE06) [58] was used to check the obstructed topology of group-IV elemental materials. The BRs are obtained by the IRVSP program [59].

APPENDIX B: BAND STRUCTURE AND EBRS DECOMPOSITION

The band structure of C, Si, Ge, and Sn have been calculated by applying the hybrid functional method as shown in Fig. 5. To determine the topological properties of the systems, we have calculated the BRs of occupied bands at

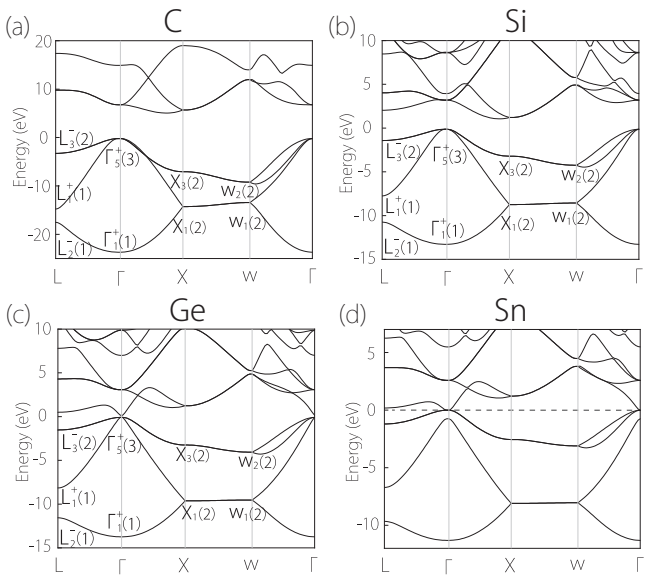

FIG. 5. (a)–(d) Band structures of group-IV elemental materials, e.g., C, Si, Ge, and Sn calculated via the HSE06 method. The BRs for each band at the high-symmetry points of C, Si, and Ge are labeled.

four high-symmetry points: L, Γ, X, and W [see labels in Figs. 5(a)–5(c)]. It can be found that C, Si, and Ge are insulators with different band gaps and have the same BRs at high-symmetry points. Thus, they can constitute same decomposable symmetry-data vector. The concept of symmetry-data vector B is defined to characterize the symmetry properties [26,60], and its explicit form is

$$B = \left\{ n_1^1 G_{K_1}^1 \oplus n_2^2 G_{K_1}^2 \oplus \ldots, n_2^1 G_{K_2}^1 \oplus n_2^2 G_{K_2}^2 \oplus \cdots \right\}, \quad \text{(B1)}$$

here, $G_{K_i}^j$ is the jth irrep of the little group at the maximal momenta K_i, and n_i^j is the multiplicity of irrep $G_{K_i}^j$. B can be decomposed on the basis of EBRs. And, the decomposition subject to

$$B = \sum_i p_i (EBR)_i. \quad \text{(B2)}$$

The topological properties of the system rely on the value of coefficient p_i [26,61]. The symmetry-data vector for X (X = C, Si, and Ge) can be written as

$$B_X = \{\Gamma_1^+(1) \oplus \Gamma_5^+(3), X_1(2) \oplus X_3(2),\ L_1^+(1) \oplus L_2^-(1) \oplus L_3^-(2), W_1(2) \oplus W_2(2)\}, \quad \text{(B3)}$$

and X belongs to the space-group $Fd3m$, which has 22 EBRs for the vspinless case (see Ref. [50]). The result of decomposition shows that coefficient $p_{(A_{1g})_{16c}\uparrow G} = 1$ and others are zero. This indicates the symmetry-data vector of X is exactly a single EBR $(A_{1g})_{16c} \uparrow G$. As a result, the Wannier charge centers of X reside at the Wyckoff position $16c$, which are mismatching with occupied Wyckoff positions ($8a$). Therefore, C, Si, and Ge are indeed OAI. In addition, one can find from Fig. 5(d) that Sn is a semimetal and is equivalent to the atomic limit case.

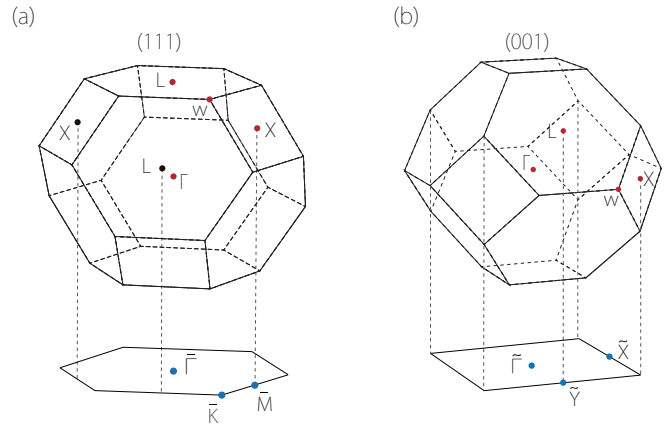

FIG. 6. Projection of bulk Brillouin zone onto (111) and (001) surfaces.

APPENDIX C: SURFACE BRILLOUIN ZONE

We now give the suface BZ and the high-symmetry points in Fig. 4 in the main text as shown in Fig. 6. Both $(111)_1$ and $(111)_2$ surfaces belong to Fig. 6(a), whereas the (001) surface belongs to Fig. 6(b).

APPENDIX D: THE ASM-TCI TRANSITION

As mentioned in the main text, an insulator derived from ASM must be a topological nontrivial insulator. Such an insulator belongs to a nontrivial phase (TI, TCI, FTI, OAI, and other phases that are not equivalent to the ASM). Here, we can take the famous TCI material SnTe as an example to study this transformation. The band structure of SnTe with SOC is presented in Fig. 7(b), which is consistent with the previous result [16]. Then we can apply tensile stress for SnTe to explore the atomic limit case. The stress applied should be large enough to ensure that the system is equivalent to the state of the atomic limit. The band structure of SnTe under a 90% tensile stress is presented in Fig. 7(a). One can clearly find that it is a ASM phase, a zoom view of the bands near the Fermi level is shown in Fig. 7(c). The number of

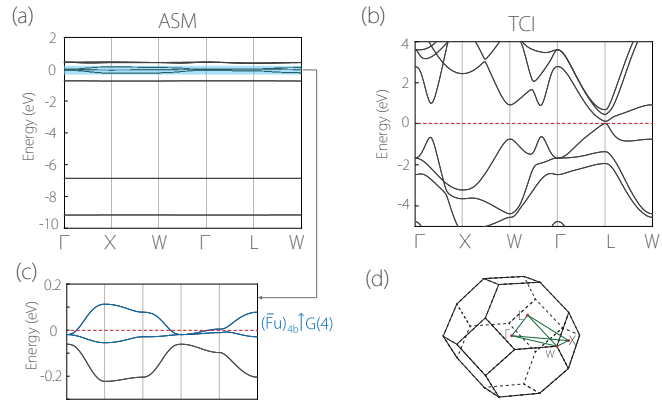

FIG. 7. The electronic structure of SnTe. (a) The band structure of SnTe under 90% tensile stress with SOC. (b) The band structure with SOC of SnTe with the fully optimized lattice constant. (c) The zoom view of the blue area in (a). (d) Bulk Brillouin zone of SnTe.

electrons is 10 in a primitive unit cell, and four sets of bands with doubly degeneracy occupied eight electrons. As a result, the remaining two electrons can not completely fill EBRs of $(\overline{F}_u)_{4b} \uparrow G(4)$ [denoted by the blue solid line in Fig. 7(c)]. This EBR was induced by the Te atom at the 4*b* Wyckoff position, and such a partially filled EBR leads to an atomic semimetal. On the other hand, we have known that SnTe is a TCI in the natural state [16]. Thus, SnTe can be used as an example from ASM to a conventional topological insulator material.

[1] X.-L. Qi and S.-C. Zhang, Topological insulators and superconductors, Rev. Mod. Phys. **83**, 1057 (2011).

[2] M. Z. Hasan and C. L. Kane, Colloquium: Topological insulators, Rev. Mod. Phys. **82**, 3045 (2010).

[3] A. Bansil, H. Lin, and T. Das, Colloquium: Topological band theory, Rev. Mod. Phys. **88**, 021004 (2016).

[4] C.-K. Chiu, J. C. Y. Teo, A. P. Schnyder, and S. Ryu, Classification of topological quantum matter with symmetries, Rev. Mod. Phys. **88**, 035005 (2016).

[5] D. J. Thouless, M. Kohmoto, M. P. Nightingale, and M. den Nijs, Quantized Hall Conductance in a Two-Dimensional Periodic Potential, Phys. Rev. Lett. **49**, 405 (1982).

[6] F. D. M. Haldane, Model for a Quantum Hall Effect without Landau Levels: Condensed-Matter Realization of the "Parity Anomaly", Phys. Rev. Lett. **61**, 2015 (1988).

[7] B. A. Bernevig, *Topological Insulators and Topological Superconductors* (Princeton University Press, Princeton, 2013).

[8] C. L. Kane and E. J. Mele, Quantum Spin Hall Effect in Graphene, Phys. Rev. Lett. **95**, 226801 (2005).

[9] B. A. Bernevig, T. L. Hughes, and S.-C. Zhang, Quantum spin Hall effect and topological phase transition in HgTe quantum wells, Science **314**, 1757 (2006).

[10] X. Wan, A. M. Turner, A. Vishwanath, and S. Y. Savrasov, Topological semimetal and fermi-arc surface states in the electronic structure of pyrochlore iridates, Phys. Rev. B **83**, 205101 (2011).

[11] R. Yu, W. Zhang, H.-J. Zhang, S.-C. Zhang, X. Dai, and Z. Fang, Quantized anomalous Hall effect in magnetic topological insulators, Science **329**, 61 (2010).

[12] Z. Qiao, S. A. Yang, W. Feng, W.-K. Tse, J. Ding, Y. Yao, J. Wang, and Q. Niu, Quantum anomalous Hall effect in graphene from Rashba and exchange effects, Phys. Rev. B **82**, 161414(R) (2010).

[13] H. Zhang, C.-X. Liu, X.-L. Qi, X. Dai, Z. Fang, and S.-C. Zhang, Topological insulators in Bi_2Se_3, Bi_2Te_3 and Sb_2Te_3 with a single dirac cone on the surface, Nat. Phys. **5**, 438 (2009).

[14] M. Wada, S. Murakami, F. Freimuth, and G. Bihlmayer, Localized edge states in two-dimensional topological insulators: Ultrathin Bi films, Phys. Rev. B **83**, 121310(R) (2011).

[15] J.-J. Zhou, W. Feng, C.-C. Liu, S. Guan, and Y. Yao, Large-gap quantum spin Hall insulator in single layer bismuth monobromide Bi_4Br_4, Nano Lett. **14**, 4767 (2014).

[16] T. H. Hsieh, H. Lin, J. Liu, W. Duan, A. Bansil, and L. Fu, Topological crystalline insulators in the snte material class, Nat. Commun. **3**, 982 (2012).

[17] H. Weng, C. Fang, Z. Fang, B. A. Bernevig, and X. Dai, Weyl Semimetal Phase in Noncentrosymmetric Transition-Metal Monophosphides, Phys. Rev. X **5**, 011029 (2015).

[18] G. Xu, H. Weng, Z. Wang, X. Dai, and Z. Fang, Chern Semimetal and the Quantized Anomalous Hall Effect in $HgCr_2Se_4$, Phys. Rev. Lett. **107**, 186806 (2011).

[19] Q. Wang, Y. Xu, R. Lou, Z. Liu, M. Li, Y. Huang, D. Shen, H. Weng, S. Wang, and H. Lei, Large intrinsic anomalous Hall effect in half-metallic ferromagnet $Co_3Sn_2S_2$ with magnetic weyl fermions, Nat. Commun. **9**, 1 (2018).

[20] Z. Wang, Y. Sun, X.-Q. Chen, C. Franchini, G. Xu, H. Weng, X. Dai, and Z. Fang, Dirac semimetal and topological phase transitions in A_3bi (a = Na, k, rb), Phys. Rev. B **85**, 195320 (2012).

[21] Z. Wang, H. Weng, Q. Wu, X. Dai, and Z. Fang, Three-dimensional dirac semimetal and quantum transport in Cd_3As_2, Phys. Rev. B **88**, 125427 (2013).

[22] Z.-M. Yu, W. Wu, X.-L. Sheng, Y. X. Zhao, and S. A. Yang, Quadratic and cubic nodal lines stabilized by crystalline symmetry, Phys. Rev. B **99**, 121106(R) (2019).

[23] A. A. Soluyanov, D. Gresch, Z. Wang, Q. Wu, M. Troyer, X. Dai, and B. A. Bernevig, Type-ii weyl semimetals, Nature (London) **527**, 495 (2015).

[24] W. Shi, B. J. Wieder, H. L. Meyerheim, Y. Sun, Y. Zhang, Y. Li, L. Shen, Y. Qi, L. Yang, J. Jena *et al.*, A charge-density-wave topological semimetal, Nat. Phys. **17**, 381 (2021).

[25] X.-P. Li, K. Deng, B. Fu, Y. K. Li, D.-S. Ma, J. F. Han, J. Zhou, S. Zhou, and Y. Yao, Type-III weyl semimetals: $(TaSe_4)_2I$, Phys. Rev. B **103**, L081402 (2021).

[26] B. Bradlyn, L. Elcoro, J. Cano, M. Vergniory, Z. Wang, C. Felser, M. I. Aroyo, and B. A. Bernevig, Topological quantum chemistry, Nature (London) **547**, 298 (2017).

[27] L. Elcoro, B. J. Wieder, Z. Song, Y. Xu, B. Bradlyn, and B. A. Bernevig, Magnetic topological quantum chemistry, Nat. Commun. **12**, 5965 (2021).

[28] H. C. Po, A. Vishwanath, and H. Watanabe, Complete theory of symmetry-based indicators of band topology, Nat. Commun. **8**, 50 (2017).

[29] H. Watanabe, H. C. Po, and A. Vishwanath, Structure and topology of band structures in the 1651 magnetic space groups, Sci. Adv. **4**, eaat8685 (2018).

[30] J. Kruthoff, J. de Boer, J. van Wezel, C. L. Kane, and R.-J. Slager, Topological Classification of Crystalline Insulators through Band Structure Combinatorics, Phys. Rev. X **7**, 041069 (2017).

[31] Z. Song, T. Zhang, Z. Fang, and C. Fang, Quantitative mappings between symmetry and topology in solids, Nat. Commun. **9**, 3530 (2018).

[32] B. Peng, Y. Jiang, Z. Fang, H. Weng, and C. Fang, Topological classification and diagnosis in magnetically ordered electronic materials, arXiv:2102.12645.

[33] A. Bouhon, G. F. Lange, and R.-J. Slager, Topological correspondence between magnetic space group representations and subdimensions, Phys. Rev. B **103**, 245127 (2021).

[34] M. Vergniory, L. Elcoro, C. Felser, N. Regnault, B. A. Bernevig, and Z. Wang, A complete catalogue of high-quality topological materials, Nature (London) **566**, 480 (2019).

[35] F. Tang, H. C. Po, A. Vishwanath, and X. Wan, Comprehensive search for topological materials using symmetry indicators, Nature (London) **566**, 486 (2019).

[36] T. Zhang, Y. Jiang, Z. Song, H. Huang, Y. He, Z. Fang, H. Weng, and C. Fang, Catalogue of topological electronic materials, Nature (London) **566**, 475 (2019).

[37] Y. Xu, L. Elcoro, Z.-D. Song, B. J. Wieder, M. Vergniory, N. Regnault, Y. Chen, C. Felser, and B. A. Bernevig, High-throughput calculations of magnetic topological materials, Nature (London) **586**, 702 (2020).

[38] H. C. Po, H. Watanabe, and A. Vishwanath, Fragile Topology and Wannier Obstructions, Phys. Rev. Lett. **121**, 126402 (2018).

[39] J. Cano, B. Bradlyn, Z. Wang, L. Elcoro, M. G. Vergniory, C. Felser, M. I. Aroyo, and B. A. Bernevig, Building blocks of topological quantum chemistry: Elementary band representations, Phys. Rev. B **97**, 035139 (2018).

[40] Z.-D. Song, L. Elcoro, Y.-F. Xu, N. Regnault, and B. A. Bernevig, Fragile Phases as Affine Monoids: Classification and Material Examples, Phys. Rev. X **10**, 031001 (2020).

[41] J. Gao, Y. Qian, H. Jia, Z. Guo, Z. Fang, M. Liu, H. Weng, and Z. Wang, Unconventional materials: the mismatch between electronic charge centers andatomic positions, Sci. Bull. **67**, 598 (2022).

[42] M. B. de Paz, M. G. Vergniory, D. Bercioux, A. García-Etxarri, and B. Bradlyn, Engineering fragile topology in photonic crystals: Topological quantum chemistry of light, Phys. Rev. Research **1**, 032005(R) (2019).

[43] S. K. Radha and W. R. L. Lambrecht, Topological obstructed atomic limit insulators by annihilating dirac fermions, Phys. Rev. B **103**, 075435 (2021).

[44] www.topologicalquantumchemistry.fr.

[45] Y. Xu, L. Elcoro, Z.-D. Song, M. Vergniory, C. Felser, S. S. P. Parkin, N. Regnault, J. L. Mañes, and B. A. Bernevig, Filling-enforced obstructed atomic insulators, arXiv:2106.10276.

[46] H. Seo, R. C. Hatch, P. Ponath, M. Choi, A. B. Posadas, and A. A. Demkov, Critical differences in the surface electronic structure of ge(001) and si(001): *Ab initio* theory and angle-resolved photoemission spectroscopy, Phys. Rev. B **89**, 115318 (2014).

[47] L. S. O. Johansson, R. I. G. Uhrberg, P. Mårtensson, and G. V. Hansson, Surface-state band structure of the Si(100)2 × 1 surface studied with polarization-dependent angle-resolved photoemission on single-domain surfaces, Phys. Rev. B **42**, 1305 (1990).

[48] Y. Aihara, M. Hirayama, and S. Murakami, Anomalous dielectric response in insulators with the π zak phase, Phys. Rev. Res. **2**, 033224 (2020).

[49] H. Watanabe, H. C. Po, M. P. Zaletel, and A. Vishwanath, Filling-Enforced Gaplessness in Band Structures of the 230 Space Groups, Phys. Rev. Lett. **117**, 096404 (2016).

[50] www.cryst.ehu.es Bilbao Crystallographic Server.

[51] J. Zak, Berry's Phase for Energy Bands in Solids, Phys. Rev. Lett. **62**, 2747 (1989).

[52] G. Kresse and J. Furthmüller, Efficiency of *ab-initio* total energy calculations for metals and semiconductors using a plane-wave basis set, Comput. Mater. Sci. **6**, 15 (1996).

[53] G. Kresse and J. Furthmüller, Efficient iterative schemes for *ab initio* total-energy calculations using a plane-wave basis set, Phys. Rev. B **54**, 11169 (1996).

[54] J. P. Perdew, K. Burke, and M. Ernzerhof, Generalized Gradient Approximation Made Simple, Phys. Rev. Lett. **77**, 3865 (1996).

[55] P. E. Blöchl, Projector augmented-wave method, Phys. Rev. B **50**, 17953 (1994).

[56] A. A. Mostofi, J. R. Yates, Y.-S. Lee, I. Souza, D. Vanderbilt, and N. Marzari, wannier90: A tool for obtaining maximally-localised wannier functions, Comput. Phys. Commun. **178**, 685 (2008).

[57] Q. Wu, S. Zhang, H.-F. Song, M. Troyer, and A. A. Soluyanov, Wanniertools: An open-source software package for novel topological materials, Comput. Phys. Commun. **224**, 405 (2018).

[58] J. Heyd, G. E. Scuseria, and M. Ernzerhof, Hybrid functionals based on a screened coulomb potential, J. Chem. Phys. **118**, 8207 (2003).

[59] J. Gao, Q. Wu, C. Persson, and Z. Wang, Irvsp: To obtain irreducible representations of electronic states in the vasp, Comput. Phys. Commun. **261**, 107760 (2021).

[60] D.-S. Ma, Y. Xu, C. S. Chiu, N. Regnault, A. A. Houck, Z. Song, and B. A. Bernevig, Spin-Orbit-Induced Topological Flat Bands in Line and Split Graphs of Bipartite Lattices, Phys. Rev. Lett. **125**, 266403 (2020).

[61] Z.-D. Song, L. Elcoro, and B. A. Bernevig, Twisted bulk-boundary correspondence of fragile topology, Science **367**, 794 (2020).